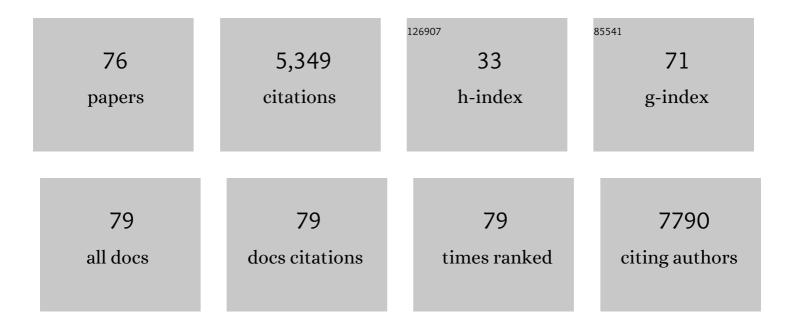
## List of Publications by Year in descending order

Source: https://exaly.com/author-pdf/913457/publications.pdf Version: 2024-02-01



#	Article	IF	CITATIONS
1	Knowledge of Hyperemic Myocardial Blood Flow in Healthy Subjects Helps Identify Myocardial Ischemia in Patients With Coronary Artery Disease. Frontiers in Cardiovascular Medicine, 2022, 9, 817911.	2.4	0
2	BoxCar and shotgun proteomic analyses reveal molecular networks regulated by UBR5 in prostate cancer. Proteomics, 2022, 22, e2100172.	2.2	2
3	Early innate immune responses in different COVIDâ€19 subâ€phenotypes through a transcriptomics lens. Clinical and Translational Discovery, 2022, 2, .	0.5	0
4	Proteome-Scale Analysis of Protein <i>S</i> -Acylation Comes of Age. Journal of Proteome Research, 2021, 20, 14-26.	3.7	19
5	Boosted Responsivity and Tunable Spectral Response in Bâ€Site Substituted 2D Ca <sub>2</sub> Nb <sub>3â^'</sub> <i><sub>x</sub></i> Ta <i><sub>x</sub></i> O <sub>10</sub> Perovskite Photodetectors. Advanced Functional Materials, 2021, 31, 2101480.	14.9	29
6	Dissecting the multi-omics atlas of the exosomes released by human lung adenocarcinoma stem-like cells. Npj Genomic Medicine, 2021, 6, 48.	3.8	18
7	Single-cell Long Non-coding RNA Landscape of T Cells in Human Cancer Immunity. Genomics, Proteomics and Bioinformatics, 2021, 19, 377-393.	6.9	15
8	Interplay and cooperation between SREBF1 and master transcription factors regulate lipid metabolism and tumor-promoting pathways in squamous cancer. Nature Communications, 2021, 12, 4362.	12.8	50
9	Supersaturationâ€Controlled Growth of Monolithically Integrated Leadâ€Free Halide Perovskite Singleâ€Crystalline Thin Film for Highâ€Sensitivity Photodetectors. Advanced Materials, 2021, 33, e2103010.	21.0	114
10	Supersaturationâ€Controlled Growth of Monolithically Integrated Leadâ€Free Halide Perovskite Singleâ€Crystalline Thin Film for Highâ€Sensitivity Photodetectors (Adv. Mater. 41/2021). Advanced Materials, 2021, 33, 2170324.	21.0	16
11	Identification of Flow-Limiting Coronary Stenosis With PCS: A New Cost-Effective Index Derived From the Product of Corrected TIMI Frame Count and Percent Diameter Stenosis. Frontiers in Cardiovascular Medicine, 2021, 8, 718935.	2.4	2
12	On the Road to Accurate Protein Biomarkers in Prostate Cancer Diagnosis and Prognosis: Current Status and Future Advances. International Journal of Molecular Sciences, 2021, 22, 13537.	4.1	11
13	Selfâ€Polarized BaTiO <sub>3</sub> for Greatly Enhanced Performance of ZnO UV Photodetector by Regulating the Distribution of Electron Concentration. Advanced Functional Materials, 2020, 30, 1907650.	14.9	74
14	Crossâ€Bar SnO <sub>2</sub> â€NiO Nanofiberâ€Arrayâ€Based Transparent Photodetectors with High Detectivity. Advanced Electronic Materials, 2020, 6, 1901048.	5.1	68
15	2D Perovskite Sr <sub>2</sub> Nb <sub>3</sub> O <sub>10</sub> for Highâ€Performance UV Photodetectors. Advanced Materials, 2020, 32, e1905443.	21.0	210
16	EWS-FL1 regulates and cooperates with core regulatory circuitry in Ewing sarcoma. Nucleic Acids Research, 2020, 48, 11434-11451.	14.5	18
17	IFI16 promotes human embryonic stem cell trilineage specification through interaction with p53. Npj Regenerative Medicine, 2020, 5, 18.	5.2	4
18	<i>S</i> -Palmitoylation as a Functional Regulator of Proteins Associated with Cisplatin Resistance in Bladder Cancer. International Journal of Biological Sciences, 2020, 16, 2490-2505.	6.4	26

#	Article	IF	CITATIONS
19	Sex as a Determinant of Responses to a Coronary Artery Disease Self-Antigen Identified by Immune-Peptidomics. Frontiers in Immunology, 2020, 11, 694.	4.8	3
20	Androgens modify therapeutic response to cabazitaxel in models of advanced prostate cancer. Prostate, 2020, 80, 926-937.	2.3	3
21	TP63, SOX2, and KLF5 Establish a Core Regulatory Circuitry That Controls Epigenetic and Transcription Patterns in Esophageal Squamous Cell Carcinoma Cell Lines. Gastroenterology, 2020, 159, 1311-1327.e19.	1.3	92
22	Comprehensive palmitoylâ€proteomic analysis identifies distinct protein signatures for large and small cancerâ€derived extracellular vesicles. Journal of Extracellular Vesicles, 2020, 9, 1764192.	12.2	37
23	Recent Progress of Heterojunction Ultraviolet Photodetectors: Materials, Integrations, and Applications. Advanced Functional Materials, 2020, 30, 1909909.	14.9	264
24	Inhibition of collagen XI alpha 1-induced fatty acid oxidation triggers apoptotic cell death in cisplatin-resistant ovarian cancer. Cell Death and Disease, 2020, 11, 258.	6.3	49
25	Proteomic profiling of bladder cancer for precision medicine in the clinical setting: A review for the busy urologist. Investigative and Clinical Urology, 2020, 61, 539.	2.0	3
26	Low-Background Acyl-Biotinyl Exchange Largely Eliminates the Coisolation of Non- <i>S</i> -Acylated Proteins and Enables Deep <i>S</i> -Acylproteomic Analysis. Analytical Chemistry, 2019, 91, 9858-9866.	6.5	32
27	Transparent Schottky Photodiode Based on AgNi NWs/SrTiO <sub>3</sub> Contact with an Ultrafast Photoresponse to Shortâ€Wavelength Blue Light and UVâ€Shielding Effect. Advanced Functional Materials, 2019, 29, 1905923.	14.9	40
28	Proteomic Analysis Identifies Membrane Proteins Dependent on the ER Membrane Protein Complex. Cell Reports, 2019, 28, 2517-2526.e5.	6.4	53
29	Low-cost writing method for self-powered paper-based UV photodetectors utilizing Te/TiO <sub>2</sub> and Te/ZnO heterojunctions. Nanoscale Horizons, 2019, 4, 452-456.	8.0	64
30	Unraveling the genetic architecture of grain size in einkorn wheat through linkage and homology mapping and transcriptomic profiling. Journal of Experimental Botany, 2019, 70, 4671-4688.	4.8	19
31	Solutionâ€Processed Transparent Sn <sup>4+</sup> â€Doped CuI Hybrid Photodetectors with Enhanced Performances. Advanced Materials Interfaces, 2019, 6, 1900669.	3.7	36
32	Millimeter-Sized Single-Crystal CsPbrB <sub>3</sub> /CuI Heterojunction for High-Performance Self-Powered Photodetector. Journal of Physical Chemistry Letters, 2019, 10, 2400-2407.	4.6	99
33	Resequencing of 429 chickpea accessions from 45 countries provides insights into genome diversity, domestication and agronomic traits. Nature Genetics, 2019, 51, 857-864.	21.4	219
34	Quantitative proteomic analysis of prostate tissue specimens identifies deregulated protein complexes in primary prostate cancer. Clinical Proteomics, 2019, 16, 15.	2.1	15
35	Keratin 8 is a potential self-antigen in the coronary artery disease immunopeptidome: A translational approach. PLoS ONE, 2019, 14, e0213025.	2.5	28
36	Siliconâ€Compatible Photodetectors: Trends to Monolithically Integrate Photosensors with Chip Technology. Advanced Functional Materials, 2019, 29, 1808182.	14.9	198

#	Article	IF	CITATIONS
37	Self-Powered Dual-Color UV–Green Photodetectors Based on SnO <sub>2</sub> Millimeter Wire and Microwires/CsPbBr <sub>3</sub> Particle Heterojunctions. Journal of Physical Chemistry Letters, 2019, 10, 836-841.	4.6	190
38	Materials and Designs for Wearable Photodetectors. Advanced Materials, 2019, 31, e1808138.	21.0	279
39	Transparent Schottky Photodiodes: Transparent Schottky Photodiode Based on AgNi NWs/SrTiO <sub>3</sub> Contact with an Ultrafast Photoresponse to Shortâ€Wavelength Blue Light and UVâ€Shielding Effect (Adv. Funct. Mater. 46/2019). Advanced Functional Materials, 2019, 29, 1970319.	14.9	1
40	Constructing the Band Alignment of Graphitic Carbon Nitride (g-C <sub>3</sub> N <sub>4</sub> )/Copper(I) Oxide (Cu <sub>2</sub> O) Composites by Adjusting the Contact Facet for Superior Photocatalytic Activity. ACS Applied Energy Materials, 2019, 2, 1803-1811.	5.1	29
41	<b>Biomarkers with Potential Predictive Value for Cardiotoxicity in Anticancer Treatments</b> . Chinese Medical Sciences Journal, 2019, 36, 1.	0.4	0
42	Efficiency enhancement of TiO <sub>2</sub> self-powered UV photodetectors using a transparent Ag nanowire electrode. Journal of Materials Chemistry C, 2018, 6, 3334-3340.	5.5	71
43	Super-Enhancer-Driven Long Non-Coding RNA LINC01503, Regulated by TP63, Is Over-Expressed and Oncogenic in Squamous Cell Carcinoma. Gastroenterology, 2018, 154, 2137-2151.e1.	1.3	165
44	Ethanol Induced Disordering of Pancreatic Acinar Cell Endoplasmic Reticulum: An ER Stress/Defective Unfolded Protein Response Model. Cellular and Molecular Gastroenterology and Hepatology, 2018, 5, 479-497.	4.5	19
45	FOXC1-induced non-canonical WNT5A-MMP7 signaling regulates invasiveness in triple-negative breast cancer. Oncogene, 2018, 37, 1399-1408.	5.9	67
46	Chromosome-level reference genome and alternative splicing atlas of moso bamboo (Phyllostachys) Tj ETQq0 0 (	Ο rgBT /Ον 6.4	erlock 10 Tf 5
47	Emerin Deregulation Links Nuclear Shape Instability to Metastatic Potential. Cancer Research, 2018, 78, 6086-6097.	0.9	49
48	Selfâ€Powered n‧nO <sub>2</sub> /p uZnS Core–Shell Microwire UV Photodetector with Optimized Performance. Advanced Optical Materials, 2018, 6, 1800213.	7.3	83
49	High-Performance Silicon-Compatible Large-Area UV-to-Visible Broadband Photodetector Based on Integrated Lattice-Matched Type II Se/n-Si Heterojunctions. Nano Letters, 2018, 18, 4697-4703.	9.1	212
50	Personalization of prostate cancer therapy through phosphoproteomics. Nature Reviews Urology, 2018, 15, 483-497.	3.8	25
51	Selfâ€Powered Ultraviolet Photodetectors Driven by Builtâ€in Electric Field. Small, 2017, 13, 1701687.	10.0	245
52	Identification of QTL and Qualitative Trait Loci for Agronomic Traits Using SNP Markers in the Adzuki Bean. Frontiers in Plant Science, 2017, 8, 840.	3.6	26
53	Recent breeding programs enhanced genetic diversity in both desi and kabuli varieties of chickpea (Cicer arietinum L.). Scientific Reports, 2016, 6, 38636.	3.3	77

54Fabrication of MnO/C composites utilizing pitch as the soft carbon source for rechargeable Li-ion<br/>batteries. New Journal of Chemistry, 2016, 40, 9986-9992.2.811

#	Article	IF	CITATIONS
55	Transcriptome and proteome characterization of surface ectoderm cells differentiated from human iPSCs. Scientific Reports, 2016, 6, 32007.	3.3	25
56	Large oncosomes contain distinct protein cargo and represent a separate functional class of tumor-derived extracellular vesicles. Oncotarget, 2015, 6, 11327-11341.	1.8	289
57	Excellent performance of carbon-coated TiO <sub>2</sub> /Li <sub>4</sub> Ti <sub>5</sub> 0 <sub>12</sub> composites with low Li/Ti ratio for Li-ion storage. RSC Advances, 2015, 5, 93155-93161.	3.6	10
58	Regulation of microtubule dynamics by DIAPH3 influences amoeboid tumor cell mechanics and sensitivity to taxanes. Scientific Reports, 2015, 5, 12136.	3.3	48
59	Targeting metabolic plasticity in breast cancer cells via mitochondrial complex I modulation. Breast Cancer Research and Treatment, 2015, 150, 43-56.	2.5	18
60	Technologies and Challenges in Proteomic Analysis of Protein S-acylation. Journal of Proteomics and Bioinformatics, 2014, 07, 256-263.	0.4	18
61	The complex jujube genome provides insights into fruit tree biology. Nature Communications, 2014, 5, 5315.	12.8	251
62	Integration of proteomic and transcriptomic profiles identifies a novel PDGF-MYC network in human smooth muscle cells. Cell Communication and Signaling, 2014, 12, 44.	6.5	24
63	Caveolin-1 and Prostate Cancer Progression. Advances in Experimental Medicine and Biology, 2012, 729, 95-110.	1.6	33
64	'Omics' Approaches to Understanding Interstitial Cystitis/Painful Bladder Syndrome/Bladder Pain Syndrome. International Neurourology Journal, 2012, 16, 159.	1.2	19
65	Integration analysis of quantitative proteomics and transcriptomics data identifies potential targets of frizzledâ€8 proteinâ€related antiproliferative factor <i>in vivo</i> . BJU International, 2012, 110, E1138-46.	2.5	14
66	Proteomic analysis of palmitoylated platelet proteins. Blood, 2011, 118, e62-e73.	1.4	105
67	Quantitative Proteomics Identifies a Î <sup>2</sup> -Catenin Network as an Element of the Signaling Response to Frizzled-8 Protein-Related Antiproliferative Factor. Molecular and Cellular Proteomics, 2011, 10, M110.007492.	3.8	31
68	Proteome Scale Characterization of Human S-Acylated Proteins in Lipid Raft-enriched and Non-raft Membranes. Molecular and Cellular Proteomics, 2010, 9, 54-70.	3.8	252
69	Quantitative Proteomics Analysis Reveals Molecular Networks Regulated by Epidermal Growth Factor Receptor Level in Head and Neck Cancer. Journal of Proteome Research, 2010, 9, 3073-3082.	3.7	26
70	Oncosome Formation in Prostate Cancer: Association with a Region of Frequent Chromosomal Deletion in Metastatic Disease. Cancer Research, 2009, 69, 5601-5609.	0.9	325
71	Rapid preparation of nuclei-depleted detergent-resistant membrane fractions suitable for proteomics analysis. BMC Cell Biology, 2008, 9, 30.	3.0	44
72	Proteomic approaches to the analysis of multiprotein signaling complexes. Proteomics, 2008, 8, 832-851.	2.2	45

#	Article	IF	CITATIONS
73	Proteomic analysis of rat pheochromocytoma PC12 cells. Proteomics, 2006, 6, 2982-2990.	2.2	30
74	Proteomic analysis and comparison of the biopsy and autopsy specimen of human brain temporal lobe. Proteomics, 2006, 6, 4987-4996.	2.2	29
75	Induction of Apoptosis in Mouse Liver by Microcystin-LR. Molecular and Cellular Proteomics, 2005, 4, 958-974.	3.8	126
76	Differential Display Proteome Analysis of PC-12 Cells Transiently Transfected with Metallothionein-3 Gene. Journal of Proteome Research, 2004, 3, 126-131.	3.7	9